

Operation track record and repair of direct electrical heating system

Kristian Solheim. Thinn¹, Jens Kristian. Lervik¹, Hallvard. Faremo¹, Katharina Kuhlefelt. Klusmeier¹, Christian Brede. Willumsen²,
Atle Harald. Børnes², Øyvind. Iversen³.

¹SINTEF Energi AS, Trondheim, Norway

²Equinor ASA, Trondheim, Norway

³Nexans Norway AS, Oslo, Norway

ABSTRACT

Direct electrical heating is a flow assurance method for subsea flowlines. This article considers direct electrically heated flowlines that were installed at an offshore facility in 2004. In 2022, one of the piggyback cables was successfully repaired. The root cause for failure was dielectric breakdown of the transition joint between the feeder cable and the piggyback cable because of high accidental axial compression forces. The accumulated operation time from 2004 to 2022 was 450 days. Fingerprints from commissioning were essential in fault location, and the fault was pin pointed with an accuracy of a few meters. Investigations of the XLPE insulation material showed that the cable was in a generally good condition.

KEY WORDS: Direct electrical heating; flow assurance; repair; fault location; operation record; prolonged lifetime.

INTRODUCTION

Direct electrical heating (DEH) is used as a flow assurance method to maintain the mixture of oil, gas and other substances in flowlines at elevated temperatures to prevent blockages from wax and hydrates. DEH is often used as an alternative to chemical inhibitors. The first DEH system installed was at the Åsgard field in 2000, followed by Huldra and Kristin, (Nysveen et al., 2005). Today, 16 fields have flowlines with DEH. These are located outside the coast of Norway (Alve, Goliat, Gullfaks Sør, Huldra, Kristin, Maria, Morvin, Urd, Skarv, Skuld, Tommeliten Alpha, Tyrihans and Åsgard), West Africa (Lianzi and Olowi) and the Caspian Sea (Shah Deniz).

In 2004, six DEH flowlines were installed at an offshore facility in the North Sea. They were 6-7 km long 10" 13Cr flowlines with U-value of 8 W/(m²K). One was never put in operation, while the others have been in operation for a shorter or longer time. In autumn 2022, a subsea fault was detected on one of the lines, called "DEH1" in this article. It was repaired in late 2022 and re-commissioned early 2023. This is the third known failure to be repaired, after Huldra (2001) and Skarv (2013) that failed because of damage occurring during installation.

This article covers several topics that are rarely published, but that gives

valuable insight into DEH systems for vendors as well as operators. First, the early design of power cables is evaluated and compared to newer designs. Second, the operation history of the five DEH flowlines is presented. Then, the design performance of the heating system is compared to actual performance. Further, the fault location methods are presented focusing on how these were actively used in the fault location campaign. Then, the offshore repair and implications on the topside system are considered. Finally, results from dissection and testing of the retrieved power cable are presented, providing new knowledge of the condition of wet-designed power cables after eighteen years submerged in seawater at 400 m depth.

ELECTRICAL SYSTEM

The topside power supply of each DEH flowline consists of a step-down three-phase power transformer (11 kV to 2.4-5.7 kV), a symmetry unit (32-58 mH, 179-311 μF) and a compensation unit (892-1553 μF). The compensation unit balances the inductance of the DEH system, resulting in a power factor close to 1.0. The purpose of the symmetry unit is to evenly distribute the single-phase load to a balanced three-phase load.

From the compensation unit, topside cables are laid to the topside junction boxes. The subsea part, see Figure 1, consists of riser cables (12 kV 1600 mm², but replaced by 24 kV 1600 mm² in 2018 due to field extension) with common metallic armor. The riser cable is a four-core (quad) cable that supplies two separate DEH flowlines.

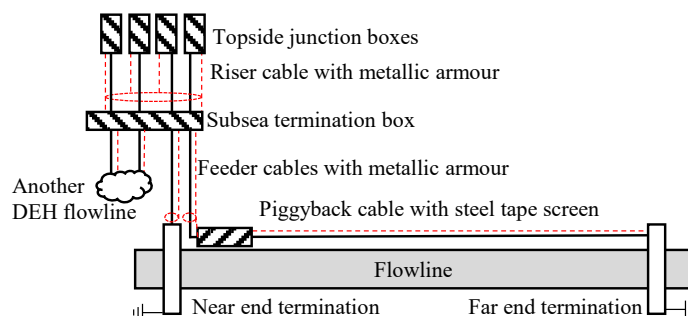


Figure 1: The DEH system.

From the subsea termination box, two single core feeder cables are routed to the near end of each flowline. One is connected to the near end termination on the flowline, while the other is spliced to a piggyback cable that is routed along the flowline and connected at the far end termination plate. The feeder cables (12 kV, 1000 mm² copper) are individual single core cables with metallic armor, see Figure 2. The piggyback cable (12 kV, 1000 mm² copper) has four metallic steel tape screens and an insulating outer sheath (jacket).

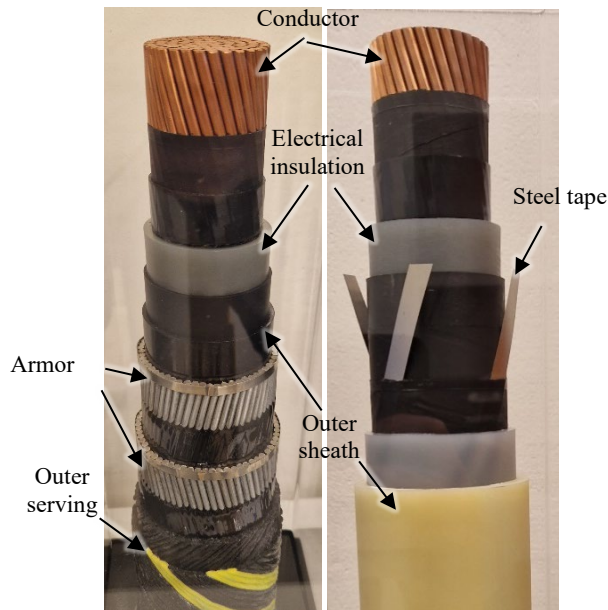


Figure 2: Feeder cable (left) and piggyback cable (right) with key components indicated.

In newer installations, the feeder and piggyback cable designs are modified. The two single core feeder cables from around around 2008 replaced with one dual core cable or one concentric designed cable in new installations. A main challenge with two individual feeder cables is that the armor of each cable carries a large current, around 70-80% of the conductor current. This adds costs due to increased heat losses, and is also a reliability concern, especially in the terminations.

For the piggyback cable, there are three main design changes from the early installations. The first is the introduction of a semiconductive outer jacket, that made the steel tape screen and outer insulated jacket superfluous. Since the sheath originally was electrically insulating, steel tapes were incorporated to conduct capacitive current from the power core. The main challenge with the steel tape is their fragility, especially in joints. Damaged tapes will over time also damage the power cable. On the other hand, the tape is beneficial for fault location by time domain reflectometer (TDR), as will be discussed later in this article. The heat loss in the tape is about 1% of total losses, that is negligible.

In the early days of DEH, the mechanical impact requirement for trawl board protection was based on a NORSOK standard with flat hammer and this was feasible to provide a sandwich design on insulating sheaths. More stringent impact requirement according to DNV RP-F111 resulted in that the power cables being placed in an external protection system. An improvement is that the protection system is now an integrated part of the power cable, see Figure 3. The protection can either have semi-conductive layers, or holes can be drilled, to allow drainage of capacitive currents.

The third improvement in newer piggyback cable designs is the

integration of fiber optics cables into the power cables. This was introduced from around 2008. These are used to improve fault detection, especially for faults located at the far end of the DEH system. In the event of burn-through, an optical time domain reflectometer (OTDR) is used to pinpoint the fault. The fiber optic can also be used to monitor power cable temperature, used for life-time estimations.

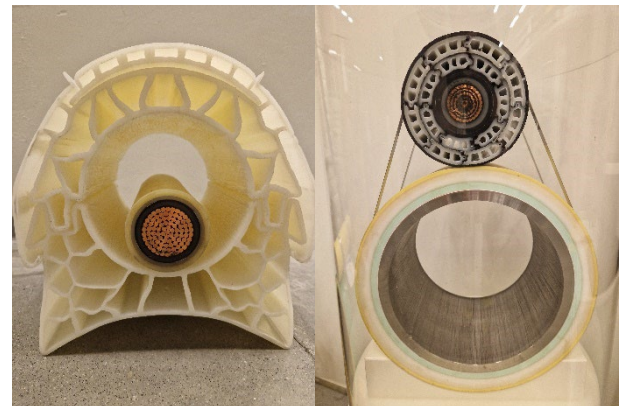


Figure 3: Cross section of piggyback cable inside mechanical protection system (left) and an integrated mechanical protection system strapped around flowline (right).

OPERATION

The five DEH systems that were installed in 2004 (DEH1, DEH2, DEH3, DEH5 and DEH6) have accumulated been operated from a few months to some years, see Figure 4. Initial design requirement was less than 2 years since it was to be used during shut-down of the production. The graphs must be considered indicative as some parts of the data are unexplainable, such as temporary reduced operation time. This may be due to various software upgrades, signal swapping, downtimes or similar. Also, the graphs start in 2008, even though the systems were put in operation in 2005.

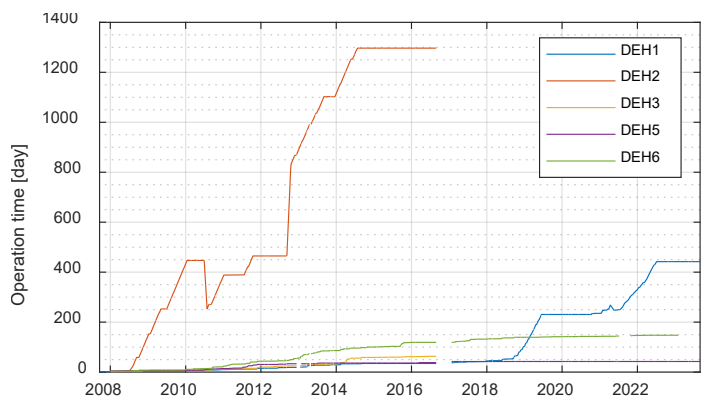


Figure 4: Accumulated operation time of DEH systems.

In Figure 5, an hourly momentary value of DEH current (% of max) is plotted. From the figure, it is seen that the DEH systems, maybe except DEH2, have to a large degree been operated intermittently. For example, DEH1 was turned on and off almost daily from mid-2021 to mid-2022. In general, electrical components are more mechanically and electrically stressed when operated intermittently than continuously.

Around 2017, there were some reconstructions. The riser (12 kV) to DEH1 was replaced with a new (24 kV) because DEH2 was decommissioned, and its riser slot overtaken by a new and longer DEH

flowline that operates at an increased supply voltage. Also, the DEH flowline never put in operation (DEH4) was decommissioned in the same period.

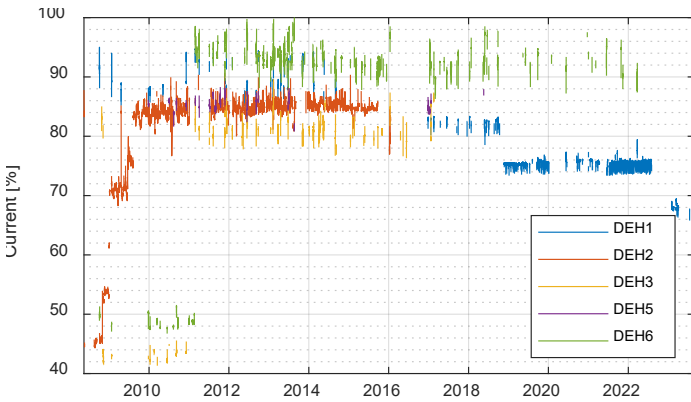


Figure 5: Applied current (% of max) in DEH systems. Momentary hourly values.

During design and operation, it is worth noticing that the DEH load resistance and reactance are temperature dependent. The temperature coefficient to electrical resistivity is 0.001 1/K for 13Cr, 0.003 1/K for X65 and 0.004 1/K for copper. For DEH1, stationary conditions are reached after about 6 hours, see Figure 6. The resistance increases by about 4%, power by 2.5%, reactance by 0.6% and current by -0.7%.

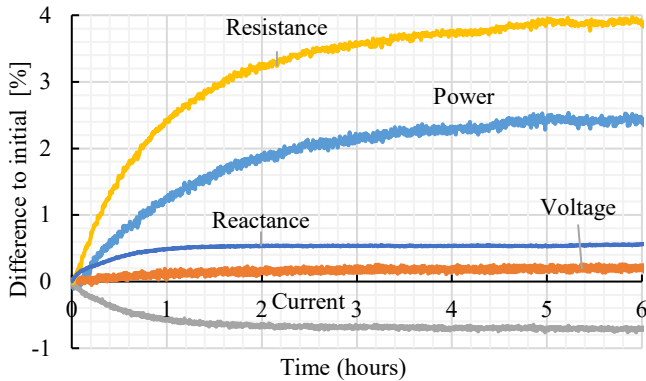


Figure 6: Record of topside parameters of DEH1 during start-up.

EVALUATION OF DEH DESIGN

The electrical impedance of the DEH system depends on several factors. A key uncertainty during design is the magnetic material properties of the steel pipe that depend on several parameters such as grit blasting, steel composition and magnetic field intensity, (Lenes et al., 2005).

This means that there is an uncertainty in every project related to the early DEH rating that is used as basis for design and procurement of the topside power system (transformer, symmetry unit and compensation unit). Therefore, a sufficient range in magnetic material properties of the steel must be accounted for in the early stage. In most projects, the magnetic properties are measured on a significant number of coated pipe sections (12 or 24 m), to improve accuracy and confidence, but these are normally first available shortly before installation.

Using DEH1 as an example, a resistivity of 0.8 $\mu\Omega\text{m}$, relative magnetic permeability of 60 and infinite correction factor (explained later) were used in design for this 13Cr pipe. Based on these values, a current (I) of

1520 A was estimated to provide a heat rate (p) of 116 W/m at a voltage (V) of 3.0 kV and total power consumption (P) of 1.2 MW, see Table 1. However, commissioning measurements indicated that the current could be reduced by 15% to produce the same power. This means that the DEH system produces more heat per ampere, which is favorable in terms of reduced total power consumption and reduced stresses of the components. Design and commissioning values agree when using permeability of 100 and correction factor (C) of 50 F.

Table 1: Design vs. actual values for DEH1 (excl. supply cables). I is current, p heat development in pipe, V supply voltage and P supply power.

Case	I [A]	p [W/m]	V [kV]	P [MW]
Design	1520	116	3.0	1.2
Actual	1320	116	2.7	1.1

The voltage and power in Table 1 do not include riser and feeder cables. These contribute to about 17% of resistance and 18% to reactance, which is considerably more than in newer installations and is mainly caused by the single core feeder cables in the old system.

Based on experience from other projects, an expected maximum variation of pipe material data for X65 is proposed in Table 2. The values can be used to sufficiently size the symmetry and compensation units. μ_r is the relative magnetic permeability of steel (dimensionless) and C the correction factor described as "Method 2" in (Lervik et al., 2007). At power frequencies of 50 Hz, a minimum value for C of 50 may be used in preference of 30, and also the experienced μ_r is lower than 1000.

Table 2: Range of electric and magnetic properties of X65 steel at 50/60 Hz. μ_r is relative magnetic permeability and C correction factor.

Description	μ_r [-]	C [F]
Base case	400	Infinite
Low R&X	250	Infinite
High R&X	1000	30

Based on magnetic steel properties proposed in Table 2, a range in the DEH impedance (resistance and reactance) is found, see Figure 7. The triangle in the center (dashed lines) represents the boundaries of experienced variation in resistance and reactance. However, design often considers all combinations of resistance and reactance, and is referred to as RX-window (resistance-reactance-window) indicated by solid lines. Impedances resulting in a lower power factor than 0.25, or 0.24 to include some margin, are not relevant for supply current greater than about 1000 A. Resistance and reactance corresponding to power factor of 0.24 is indicated by a dotted line. Power factor (pf) is defined as resistance divided by impedance.

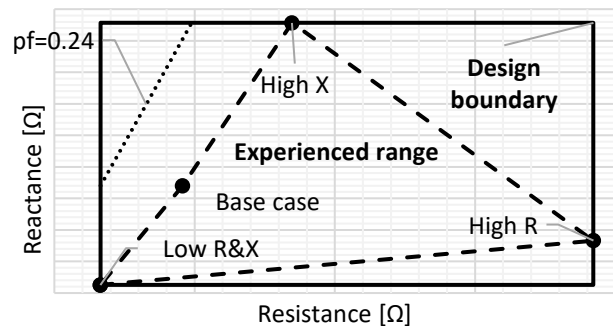


Figure 7: Generic resistance-reactance (RX)-diagram based on material data from Table 2. Power factor (pf) of 0.24 indicated by dotted lines.

It is worth mentioning that for all DEH systems to date, the key electrical

parameters (current, voltage and power) have been within design. In a few fields, the compensation unit reactor has been on the design border in systems with high resistance, i.e., high heat input per ampere.

FAULT LOCATION

Fault detection of the subsea part of DEH systems is complicated because the far end is connected to seawater. This means that a potential fault gives a second connection to ground. Hence, the number of available fault detection methods are limited (Bruaset and Kulbotten, 2011) and not necessarily as accurate as on conventional subsea power cables.

In the fault location campaign of DEH1, mainly two methods were used: impedance measurements and time domain reflectometer.

Impedance

The impedance, as seen by the topside system, consists of the topside cables (t), riser cables (r), feeder cables (f) and piggyback cable incl. flowline (DEH). This adds up to Eq. 1 where Z is impedance (Ω), z impedance per length (Ω/km) R resistance (Ω), L length to fault (km) and L_{PBC} total length of piggyback cable. Based on the known healthy impedance, the true DEH impedance (Z_{DEH}) is found, as impedances of the topside, riser and feeder cables are well known (and as described earlier, the true magnetic properties of the steel are only estimated). Proper measurements of the topside impedance for a healthy system at various voltages, including low voltage, are essential for fault location.

$$Z_{\text{healthy}} = Z_t + Z_r + Z_f + Z_{DEH} \cdot L = 0.83 + j2.30 \Omega \quad (1)$$

In the event of a ground fault on the piggyback cable, the circuit diagram becomes as in Figure 8. The fault is a parallel resistance to the impedance of DEH system downstream of the fault. The fault equation then becomes as indicated in Eq. 2. There are two unknowns in the single equation: the length to the fault and resistance (size) of the fault.

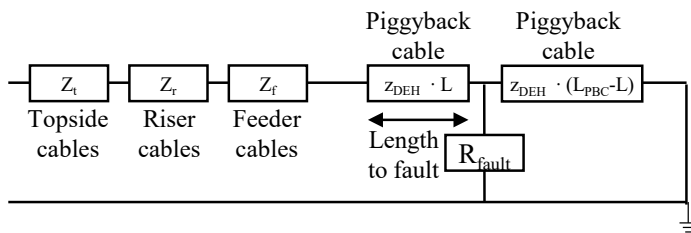


Figure 8: Circuit diagram for fault detection by impedance measurements.

$$R_{\text{faulty}} + j \cdot X_{\text{faulty}} = Z_t + Z_r + Z_f + Z_{DEH} \cdot L + R_{\text{fault}} \parallel [Z_{DEH} \cdot (L_{PBC} - L)] = 1.26 + j1.67 \Omega \quad (2)$$

Fault location is performed by considering various fault locations and fault sizes, see Figure 9 and Figure 10. In the figures, the dashed lines represent the true resistance and reactance as measured from the topside power cabinet at low voltage at the fault event. The correct size and location of the fault is found when any of the solid lines crosses the dashed lines, for both resistive and reactive terms. For DEH1, this was at $X=0$ km for a 5Ω fault (25 cm^2). $X=0$ means at the start of piggyback cable, or upstream of this location, i.e. on feeder or riser cable.

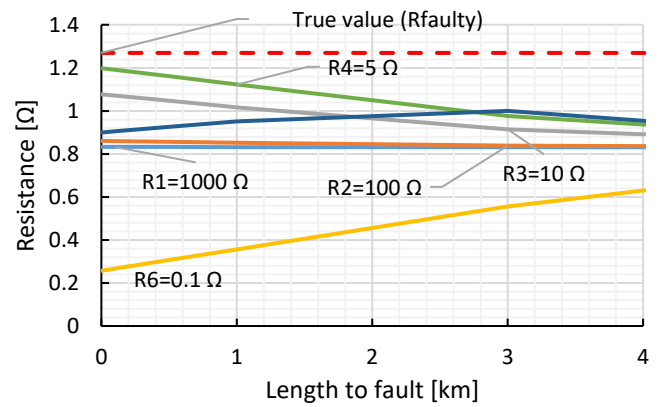


Figure 9: Topside resistance as function of length to fault for various fault types. Dashed line represents true resistance.

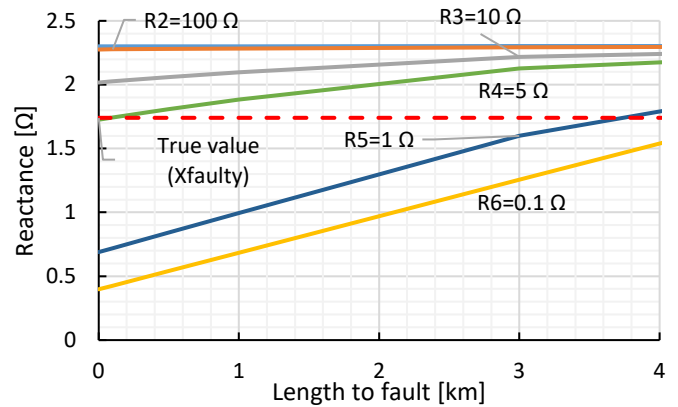


Figure 10: Topside reactance as function of length to fault for various fault types. Dashed line represents true resistance.

Time domain reflectometer (TDR)

TDR is an electronic instrument used to determine the characteristics of electrical lines by observing reflected voltage waveforms. For an ideal fault with zero ground resistance, fault location is clearly indicated by the instrument. This is however rarely the case and is why proper fingerprints are essential for fault location with TDR.

For DEH1, the raw files of the TDR fingerprints from commissioning were available from the cable vendor. With this, the new and original traces could be viewed on the same screen. The fault is located where the two traces differ: just in the vicinity of the joint reflection (vertical brown line) at about 1.6 km from topside, see Figure 11.

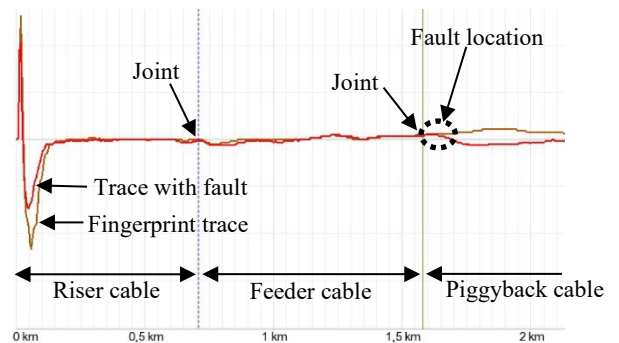


Figure 11: TDR trace of DEH1 with and without fault.

Location

The fault location was visually confirmed by ROV operation to be on the piggyback cable close to the joint between the feeder and piggyback cable, see Figure 12.



Figure 12: Fault located on piggyback cable.

SYSTEM AFTER REPAIR

During repair, some length to each side of the fault was removed and a spare piggyback cable of 800 m was spliced in in both directions: for the section where there was a piggyback cable and as a replacement of armored feeder cable since the fault was at the intersection between these. As the piggyback cable has no metallic armor, two 800 m 240 mm² ground cables were installed as continuation from the feeder cable armor to the grounding point at the pipe near end. The two main implications of the repair were an adjusted impedance and possible local reduced heating efficiency.

The resistance and reactance of the repaired system became 5 and 20 % higher, respectively, because of the repair. The main implication is that, for a fixed topside voltage, the current and consequently the power, are reduced. This means that a higher supply voltage is required to provide the same power. Also, the compensation and symmetry units had to be recoupled to reduce asymmetry in the topside three-phase network.

The second implication was a potential reduction in local heating efficiency. As the repaired piggyback cable is not strapped to the flowline, just laid next to it, the separation between them may increase locally. When the cable is placed further away from the flowline, the magnetic coupling and consequently heat development in the pipe are reduced. As the pipe is electrically insulated from seawater apart from at the ends (no intermediate anodes on 13Cr steel), there is no reduction in the overall current that is conducted by the flowline in this section, compared to the main DEH section. For an increased local flowline-cable separation of 100 cm, see Figure 13, heat development in the pipe is reduced to 89%.

On the other hand, if the separation between flowline and cable were 100 cm in a “sufficiently long” corridor (not quantified), and the flowline was connected to seawater by anodes, the heating efficiency in this section would drop to about 60%, (Lervik et al., 1998).

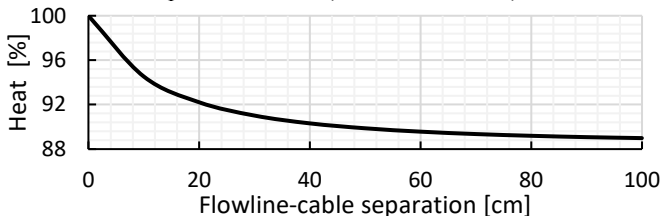


Figure 13: Heat reduction as function of flowline-cable separation.

For repair of DEH1, only very local increased offset was observed during installation, meaning that reduced heating efficiency could be neglected.

CABLE ANALYSIS

Analyses of photos from ROV and dissection of retrieved faulty piggyback cable shows that there was a dielectric breakdown close to the joint between the feeder and piggyback cable, see Figure 14. The failure was likely related to high accidental mechanical axial compression forces close to the joint. As the system was turned on almost daily until failure in 2023 this will result in repeated compression forces. It is possible that the fragile metallic screen bands have broken and accelerated cable degradation, mainly because of their sharp edges or small arcing across a broken screen band.



Figure 14: Dielectric fault of piggyback cable.

Some meters from the fault location, the steel bands holding the piggyback cable protection system to the flowline had snapped, see Figure 15. This may be a combination of thermal stresses from intermittent operation, unfortunate back-tension of piggyback cable during installation (too much cable in the protection) and other factors.



Figure 15: Piggyback cable protection snapped from flowline.

Some parts of the cable XLPE insulation close to the joints were thoroughly tested for water treeing, thermal history and oxidation. The tests showed that the cable generally was in good condition. Water ingress was not detected in the piggyback conductor, even as close as 20 m to the fault location.

A bow-tie tree indicated by an arrow in Figure 16 was 350 μm long, that is approximately 10% of the insulation thickness, but is not dangerous for the service performance of a 12 kV XLPE cable.

This is in accordance with other tests that have qualified wet design cable for at least 35 years operation, (Floden and Bengtsson, 2015).

The thermal history of the XLPE cable insulation was checked by DSC (Differential Scanning Calorimetry), and temperatures were found to be a maximum of 75°C. This is considerably lower than the 90°C thermal limit and ageing tests carried out at temperatures up to 128°C during qualification of this specific cable.

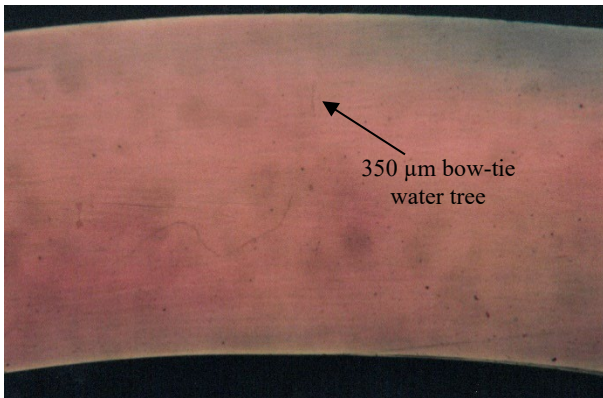


Figure 16: XLPE insulation of DEH1 piggyback cable.

Oxidation of the XLPE insulation material was checked by FTIR (Fourier Transformed Infrared) spectroscopy, based on the same method as (Hvidsten et al., 2005). These results, see Figure 17, show that the oxidation of this cable was low compared to (Hvidsten et al., 2005), meaning that the XLPE insulation in general was in good condition when the fault occurred.

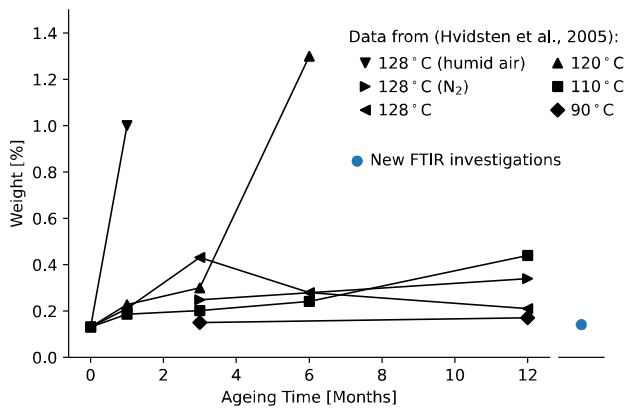


Figure 17: Carbonyl content calculated from the FTIR compared to measurements in (Hvidsten et al., 2005).

CONCLUSIONS

This article considers experience from five 18 years old DEH systems and from repair of a piggyback cable in 2023.

- The electrical design of the subsea power cables has over time improved and become more robust.
- The power cables have been operating from a few months to some years. A main part of the operation was intermitted use (many on-offs)
- The heating system has been operated in a significantly different manner than was the design condition.
- A dielectric fault was located with an accuracy of a few meters. The main methods used were low voltage impedance measurements and time domain reflectometer (TDR).
- Proper fingerprints of a healthy system are essential for fault location.
- The failure was likely related to accidental high mechanical axial compression forces close to the joint (above design values).
- Some parts of the cable XLPE insulation were thoroughly tested and showed that the cable was generally in good condition.

Bruaset, A, and Kulbotten, H (2011). "Fault Protection On Direct Electrical Heating Cables," *The Twenty-first International Offshore and Polar Engineering Conference*, Hawaii, ISOPE

Floden, R, and Bengtsson, M (2015). "Wet Ageing of XLPE Cables–Lifetime Prediction," *The Twenty-fifth International Ocean and Polar Engineering Conference*, Hawaii, ISOPE.

Hvidsten, S, Floden, R, Olafsen, K and Lundegaard, L (2005). "Long term electrical properties of XLPE cable insulation system for subsea applications at very high temperatures," *Annual Report Conference on Electrical Insulation and Dielectric Phenomena*, CEIDP'05, IEEE, 265–268.

Lenes, A, Lervik, J-K, Kulbotten, H, Nysveen, A, Børnes, A-H (2005). "Hydrate prevention on long pipelines by direct electrical heating," *The Fifteenth International Offshore and Polar Engineering Conference*, Seoul, ISOPE.

Lervik, J-K, Ahlbeck, M, Raphael, H, Lauvdal, T, Holen, P (1998). "Direct electrical heating of pipelines as a method of preventing hydrate and wax plugs," *Eighth International Offshore and Polar Engineering Conference*, Montreal, ISOPE.

Lervik, J-K, Børnes, A-H, Nysveen, A, Høyer-Hansen, M (2007). "Electromagnetic modelling of steel pipelines for DEH applications," *The Seventeenth International Offshore and Polar Engineering Conference*, Lisbon, ISOPE.

Nysveen, A, Kulbotten, H, Børnes, A-H, Hoyer-Hansen, M, (2005). "Direct electrical heating of subsea pipelines-technology development and operating experience," *Record of Conference Papers Industry Applications Society 52nd Annual Petroleum and Chemical Industry Conference*, Denver, IEEE, 177-187.